# RESEARCH ARTICLE

**Key Points:**
- From 2001 to 2015 DC measurements were made in up to 58 distinct transformers in South Island, NZ
- Stray HVDC Earth return currents and calibration problems have been corrected to produce a GIC data set
- H prime is the best correlated driver of observed GIC magnitude but not for every storm in every location

**Correspondence to:**
C. J. Rodger,
crodger@physics.otago.ac.nz

# Long-term geomagnetically induced current observations in New Zealand: Earth return corrections and geomagnetic field driver

Daniel H. Mac Manus[1], Craig J. Rodger[1] (iD), Michael Dalzell[2] (iD), Alan W. P. Thomson[3], Mark A. Clilverd[4] (iD), Tanja Petersen[5], Moritz M. Wolf[6] (iD), Neil R. Thomson[1] (iD), and Tim Divett[1] (iD)

[1]Department of Physics, University of Otago, Dunedin, New Zealand, [2]Transpower New Zealand Limited, Wellington, New Zealand, [3]British Geological Survey, Nottingham, UK, [4]British Antarctic Survey (NERC), Cambridge, UK, [5]GNS Science, Lower Hutt, New Zealand, [6]Department of Applied Sciences and Mechatronics, Munich University of Applied Sciences, Munich, Germany

**Abstract** Transpower New Zealand Limited has measured DC currents in transformer neutrals in the New Zealand electrical network at multiple South Island locations. Near-continuous archived DC current data exist since 2001, starting with 12 different substations and expanding from 2009 to include 17 substations. From 2001 to 2015 up to 58 individual transformers were simultaneously monitored. Primarily, the measurements were intended to monitor the impact of the high-voltage DC system linking the North and South Islands when it is operating in "Earth return" mode. However, after correcting for Earth return operation, as described here, the New Zealand measurements provide an unusually long and spatially detailed set of geomagnetically induced current (GIC) measurements. We examine the peak GIC magnitudes observed from these observations during two large geomagnetic storms on 6 November 2001 and 2 October 2013. Currents of ~30–50 A are observed, depending on the measurement location. There are large spatial variations in the GIC observations over comparatively small distances, which likely depend upon network layout and ground conductivity. We then go on to examine the GIC in transformers throughout the South Island during more than 151 h of geomagnetic storm conditions. We compare the GIC to the various magnitude and rate of change components of the magnetic field. Our results show that there is a strong correlation between the magnitude of the GIC and the rate of change of the horizontal magnetic field ($H'$). This correlation is particularly clear for transformers that show large GIC current during magnetic storms.

## 1. Introduction

Geomagnetic storms are potentially hazardous to the activities and technological infrastructure of modern civilization. The largest storms are triggered when coronal mass ejections (CME) from the Sun impact the Earth's magnetic field [*Gopalswamy*, 2009; *Howard*, 2011]. The reality of this hazard was dramatically demonstrated during the great magnetic storm of March 1989, when geomagnetically induced currents (GIC), driven by the time-varying geomagnetic field with the Earth's surface layers, caused the collapse of the Hydro-Québec electrical power grid in Canada. Protective relays were tripped, the grid failed, and about 9 million people were left without electricity [*Bolduc*, 2002]. The blackout lasted around 9 h for most places, but some locations were without power for days. To date, this has been the most significant power system event known to have been caused by GIC. Nonetheless, it is hardly unique, with an August 1989 storm causing the closure of the Toronto Stock Exchange [*Dayton*, 1989], the world's largest oil, gas, and mining exchange, causing significant knock-on impacts globally.

Initially, the focus on GIC effects was at high latitudes, particularly in North America and Scandinavia. In the last decade, however, there has been growing evidence of GIC impacts at low and middle latitudes, including the United Kingdom [*Erinmez et al.*, 2002], South Africa [*Koen and Gaunt*, 2003], New Zealand [*Béland and Small*, 2004], Brazil [*Trivedi et al.*, 2007], China [*Liu et al.*, 2009], and Japan [*Watari et al.*, 2009a]. Recently, significant magnetic field rates of change have been found in equatorial latitudes at CME arrival times, where the local magnetic signature is amplified by the equatorial electrojet [*Carter et al.*, 2015, 2016]. These studies have suggested that the local amplification substantially increases the equatorial region's susceptibility to GIC's, although we are unaware of direct GIC observations or GIC-linked damage reported in that zone, to date.

Work undertaken in South Africa has demonstrated increased transformer problems after large geomagnetic storms resulting in transformer deterioration and eventual failure [*Gaunt and Coetzee*, 2007]. In New Zealand there has been historic industry-supported research on GIC effects on long fuel pipelines since the mid-1970s [e.g., *Ingham*, 1993]. GIC damage to the New Zealand electrical grid has also occurred, as detailed below.

On 6 November 2001 at 14:53 New Zealand Daylight Time (NZDT, equivalent to 1:53 UT) alarms from transformers across the South Island were received by the network operator, Transpower New Zealand Ltd. Simultaneously, the voltage control equipment for Christchurch city tripped along with a transformer feeding Dunedin city. One of the phases of Dunedin/Halfway Bush transformer number 4 (referred to as HWB T4) failed within 1 min of the GIC onset time. An internal inspection revealed that the transformer was beyond repair, and it was subsequently written off. This event has been described qualitatively in the scientific literature [*Béland and Small*, 2004] and was subsequently analyzed in detail [*Marshall et al.*, 2012], albeit with degraded time resolution of the GIC data.

As described by *Marshall et al.* [2012], the South Island of New Zealand has an unusually large number of locations where quasi-DC currents are measured at earthing points of the primary AC electrical transmission network. It is common in GIC research for measurements to be limited to a single location (e.g., Japan [*Watari et al.*, 2009a], South Africa [*Lotz et al.*, 2016], or Ireland [*Blake et al.*, 2016]), or a small number of measurements at separate transformers (e.g., three to five locations in Finland [*Viljanen and Pirjola*, 1994; *Beck*, 2013] and four locations in Scotland [*Thomson et al.*, 2005]). The majority of the quasi-DC current measurements in New Zealand are made to monitor stray currents entering the AC transmission network during the Earth return operation of the high-voltage DC (HVDC) link joining the South and North Islands. In many cases multiple transformers in the same substation are independently monitored. In recent years additional measurements have been added with the specific goal of Space Weather-focused GIC monitoring.

In this study we describe the near-continuous data set of quasi-DC current measurements available from the South Island Transpower New Zealand electrical network. We describe the HVDC link and how the stray HVDC currents can be removed from the quasi-DC current measurement's to provide a very large GIC data set. We describe this process in detail as it is likely that GIC measurements in other parts of the world are similarly affected by any HVDC link they may have in operation. We present what is potentially the largest GIC data set in the world, in terms of spatial measurement density and the time length of essentially continuous operation. We demonstrate how the GIC can vary significantly across the monitored transformers and substations, by considering the geomagnetic storm of 6 November 2001, at the highest time resolution available. Finally, we examine the suggestion of *Watari et al.* [2009a, 2009b] that GIC observed at midlatitudes or affected by proximity to the coast might show a better correlation coefficient with the magnitudes of the magnetic field components, rather than the rate of change of the magnetic field.

## 2. Experimental Data Sets

### 2.1. New Zealand DC Observations

New Zealand's power network is owned and operated by Transpower New Zealand Limited. In the South Island 98% of the electricity generation comes from hydroelectricity. This is due to the large number of rivers, making the South Island an ideal location for hydroelectricity generation. However, as 75% of the population lives in the North Island a means of delivering this hydrogeneration capacity to the North Island was needed, especially during times of peak consumption. To achieve this, a HVDC link was established in 1965, connecting the North Island with the South Island. It starts from the Benmore hydroelectric power station in the South Island to the Haywards transmission substation in the lower North Island. At these locations AC-DC converters connect the AC transmission network in both islands to the HVDC link. The route of the HVDC link is shown in the Transpower South Island network diagram, Figure 1, by the heavy purple line running up the east coast of the island from Benmore (in the lower third of the island), northward. This is a total of 611 km of transmission distance including 37 km of overhead line in the North Island, 534 km of overhead line in the South Island, and a 40 km submarine cable across the Cook Strait [*Transpower*, 2010]. The original HVDC link was 250 kV, upgraded to 350 keV (for only one of the two conductors, in this case conductor number 2) and 270 kV (conductor number 1) in 1990, and to 350 kV (both conductors) in 2013. Power can be transmitted in both directions across the HVDC link allowing the North Island access to the hydrogeneration produced in the South
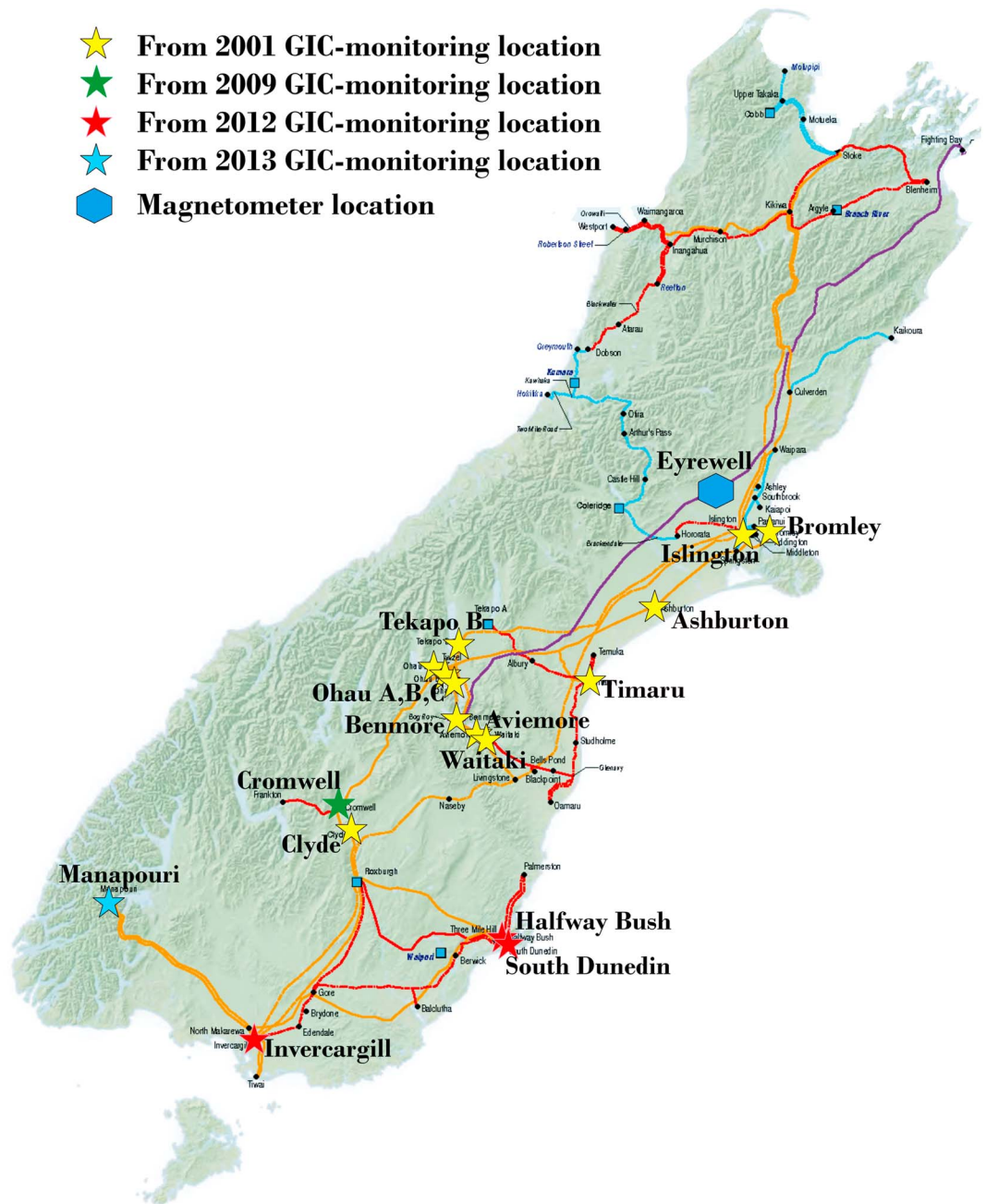
**Figure 1.** Map of the South Island of New Zealand showing the Transpower New Zealand electrical transmission network. The heavy purple line is the HVDC transmission line linking the South Island and North Island electrical networks. The other colored lines in this figure show the routes of the Transpower transmission lines, with different colors representing different voltages (orange = 220 kV, red = 110 kV, and light blue = 50/66 kV). Stars show the location of substations containing the LEM model LT 505-S DC monitoring equipment, the data from which can be corrected to produce GIC measurements. Substations without DC monitoring equipment are shown by the small blue squares. The location of the primary New Zealand magnetic observatory, Eyrewell, is given by the blue hexagon.

Island while also providing the South Island access to the North Island's thermal generation (the latter occurs mainly during dry years).

The New Zealand HVDC system usually operates as a bipole with equal current traveling on the transmission conductors between Haywards and Benmore. However, it is not uncommon for the system to operate in "Earth return" or "monopolar" mode, i.e., using a single wire and the ground. A schematic of the current
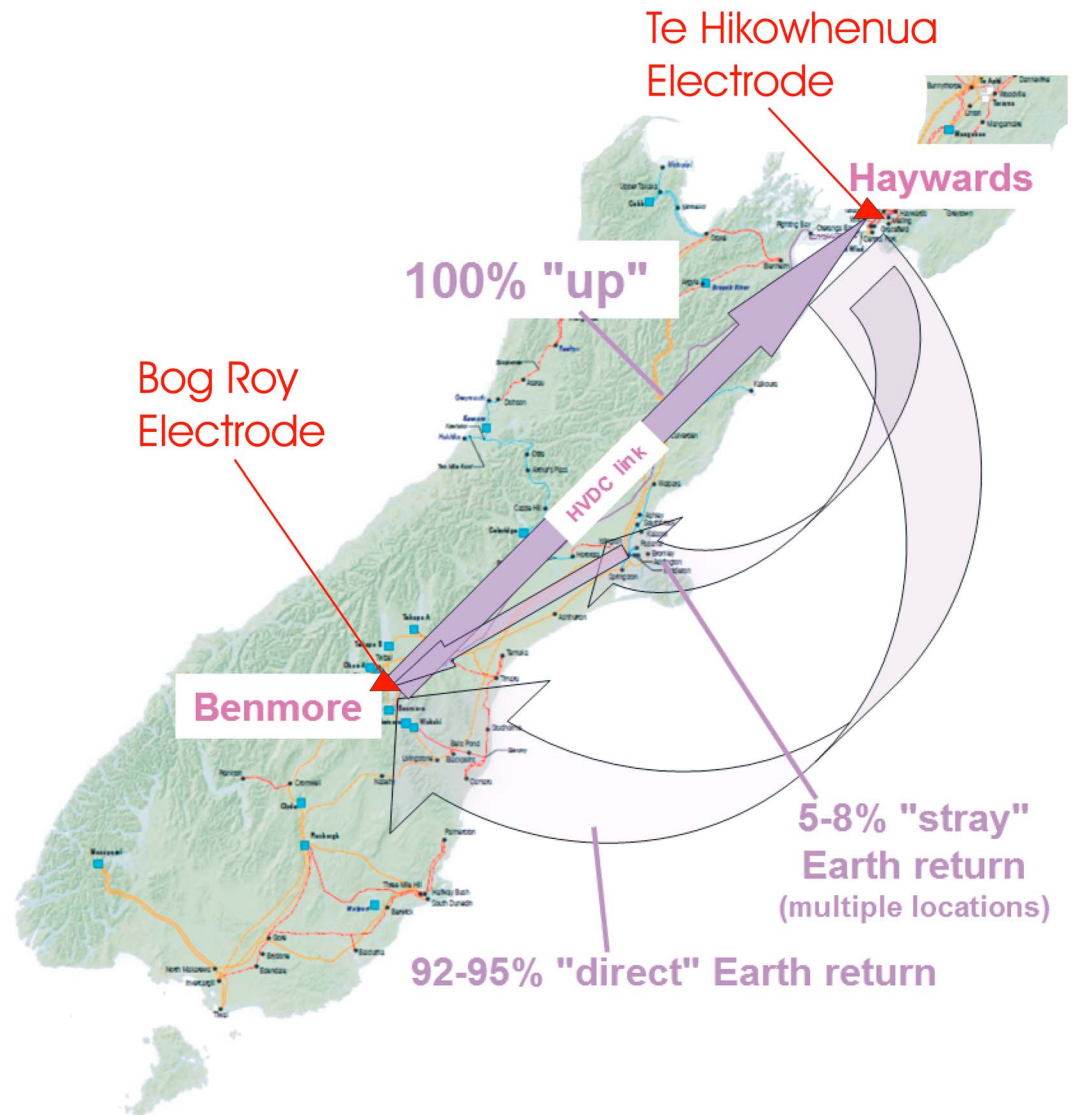
**Figure 2.** Map of the South Island and lower North Island electrical transmission network (colored lines). A schematic has been added showing the operation of the HVDC link in Earth return mode (arrows). Dark arrows are above ground; lighter arrows are below ground. A single transmission circuit links Benmore and Haywards allowing current to flow between the islands. Most of the HVDC return current passes directly between the electrodes (marked by red triangles) through the ground. The remaining fraction also travels partly through the ground but enters the transmission network through one of multiple substations, completing the loop to Benmore as DC current passing through the AC transmission network.

loop for Earth return mode is shown in Figure 2. In this case the return current passes through the ground itself to complete the loop; to enable Earth return operation, electrodes have been installed at Te Hikowhenua (at Makara, near Haywards in the North Island) and Bog Roy (near Benmore in the South Island). The locations of these electrodes are shown by red triangles in Figure 2. All of the return current travels through the Earth between those two electrodes. However, a small fraction of the current finds paths traveling from the northern electrode to the earthing points of network transformers in much of the South Island and then completing the circuit across the AC transmission lines. We term this "stray" return current. Transpower has installed DC current measuring devices (referred to as Liaisons Electroniques-Mécaniques (LEMs)) on all the transformers for which significant stray HVDC return current is expected, as those currents might lead to voltage control issues, transformer damage, or incorrect protection operation in the power system. LEM measurements have been used in the past to better understand the coupling of stray HVDC return currents into the AC transmission network [*Dalzell*, 2011].

**Table 1.** Change With Time in the Number of South Island Transformers and Substations for Which DC Monitoring Systems Were Operating at Locations Shown in Figure 1[a]

| Date | Total Transformers Monitored | Total Substations Monitored |
|---|---|---|
| Nov 2001 | 36 | 12 |
| Jan 2005 | 37 | 12 |
| Apr 2005 | 39 | 12 |
| Sep 2008 | 40 | 12 |
| Mar 2009 | 42 | 13 |
| May 2009 | 43 | 13 |
| Jul 2010 | 44 | 13 |
| Nov 2011 | 45 | 13 |
| Sep 2012 | 44 | 13 |
| Oct 2012 | 49 | 16 |
| Dec 2012 | 48 | 16 |
| Feb 2013 | 56 | 17 |
| May 2013 | 57 | 17 |
| Aug 2013 | 56 | 17 |
| Jan 2014 | 57 | 17 |
| Jun 2015 | 58 | 17 |

[a]Note that over the entire time period, 61 distinct transformers were monitored.

The GIC monitoring devices are Hall effect current transducers (LEM model LT 505-S), installed onto the transformer neutral line connection to Earth. LEM is the company name that produces the sensors (Liaisons Electroniques-Mécaniques), and the devices are commonly referred to as "LEM's" by Transpower. Datasheets for several versions of this model transducer can be found online. The version used by Transpower has primary nominal RMS current ($I_{PN}$) of 500 A and data set sheet code number 070807/8. The accuracy of the LEM model LT 505-S current measurements is ±0.6%, i.e., ±0.3 A for a 50 A value.

The locations of the substations with the original monitoring equipment are shown as yellow stars in Figure 1. At the start of the data archive available to us (November 2001), 12 sites were being monitored. LEM are located at transformers at both generation sites and substations, in many cases multiple transformers at the same location are instrumented, such that 36 sensors were deployed in 2001. Table 1 indicates how the number of transformers and substations monitored with LEM sensors has varied with time. This number initially increased slowly, with measurements being made at 36–40 transformers in 12 distinct locations until 2009. However, additional LEM began to be installed at additional substations with a specific focus of monitoring during Space Weather events (shown as green, red, and then blue stars in Figure 1). The expansion included measurements at the Halfway Bush (HWB) substation and specifically the transformer HWB T4 which had been replaced after the 6 November 2001 storm. By February 2015 a total of 58 transformers were being monitored at 17 distinct locations. The archived data are intermittent in 2001 but are essentially continuous from 2012 to the end of the period available to us (currently the end of 2015). The time resolution of the LEM DC measurement data available to us is determined by the dynamic time resolution used by the archiving software. This degrades the time resolution of the data set when the DC values are changing slowly but stores high time resolution data when the DC values are changing. In practice, this means that during geomagnetic storms when GIC are present the data have the highest time resolution (4 s), while at other times when the values are slowly changing the time resolution can be considerably longer (as much as 1 h 1 min).

Operation of the HVDC link in Earth return mode is common, and so the stray return currents must be removed from the LEM observations in order to study GIC. This is described in more detail in section 3.

### 2.2. Magnetometer

The Eyrewell (EYR) geomagnetic observatory is located at West Melton, as plotted in Figure 1. EYR is part of INTERMAGNET (http://www.intermagnet.org/) and is operated by GNS Science, New Zealand. This station provides 1 min magnetic field data with coordinates X (positive to geographic north), Y (positive to the east), and Z (positive vertically downward) to the INTERMAGNET collaboration, with a resolution of 0.1 nT. Absolute magnetic field measurements are provided by a DI-fluxgate magnetometer and a proton precession magnetometer. Note that EYR is located near the HVDC link (~20 km from EYR), as shown in Figure 1. Corrections are made to the EYR magnetic field observations to correct for HVDC operation. We have undertaken manual data quality checks of the EYR operation when there are large changes in the HVDC Earth return current levels and could see no evidence of any remaining contamination during periods of HVDC operation.

## 3. Correction for HVDC Operation

HVDC systems are relatively common for long distance power transfer, with roughly 140 large-scale systems in operation globally [*Rajgor*, 2013]. Some systems are designed from the outset as monopolar, i.e., using single wire with Earth return (e.g., the Kontek HVDC connection between Denmark and Germany and the majority of the HVDC links across the Baltic Sea [*Söderberg and Abrahamsson*, 2001]), or metallic return (e.g., Basslink interconnector between Tasmania and mainland Australia). Appendix A of *Ardelean and Minnebo* [2015] lists 36 major existing submarine HVDC cables as well as their monopole/bipolar status, with another 14 major submarine cables planned. Note that most monopole HVDC links use metallic return conductors and not Earth return.

The New Zealand HVDC link is of the bipolar type but commonly operates in Earth return mode (i.e., monopole), which will potentially affect whether the measured transformer Earth currents are caused by GIC or instead by HVDC stray currents. A similar issue was mentioned in a study into GIC in China, where current peaks were seen outside the time of a magnetic storm [*Liu et al.*, 2008] and identified as being due to HVDC operation. The magnitude of the HVDC stray current arriving at a given transformer depends upon the total HVDC current, the electrical conductivity of the ground and of the transmission network, and the location of the transformer. It seems reasonable to assume that the gross electrical structure of the ground and electrical conductivity of the network will not change significantly within a short time period, and thus, there should be a linear relationship between the total HVDC current and the stray current at a given transformer. We will later show that this is an appropriate assumption for New Zealand, where the South Island grid has not changed significantly in the time period considered.

The New Zealand HVDC link typically transmits ~150–1000 A of current through the Earth return path. We use the current measured at Benmore to provide a measure of the total HVDC Earth return current. We limit ourselves to periods where the absolute HVDC current is >100 A to investigate the significance and removal of the HVDC stray return currents. Table 2 summarizes the average yearly operation of the HVDC link. In most years the link carries >100 A in Earth return mode approximately half the time; the remainder of the time is in bipolar mode, or there is no HVDC operation. From 2008 to 2012 the HVDC link was almost continuously operating in Earth return mode (i.e., 94–100% of the time). From September 2007 one of the two conductors (termed "poles," in this case Pole 1) in the HVDC link could only be operated under restricted conditions. From that time Pole 1 was partially and later fully decommissioned, replaced in August 2013. During this period, the restriction placed on Pole 1 meant that the HVDC link was almost entirely running in single wire Earth return mode (i.e., monopolar) with only Pole 2 used. As seen in Table 2, this period is also associated with higher average total Earth return currents, as only one conductor was in use requiring 100% Earth return operation.

As noted previously, for an unchanging network configuration, there should be a linear relationship between the stray HVDC return current and the total HVDC Earth return current. An example of this is shown in Figure 3a, which presents the LEM reported current at Timaru transformer 5 (TIM T5) against the total HVDC Earth return current during the time period from the start of 8 January 2010 to the end of 14 January 2010. Periods when the absolute value of the HVDC Earth return current are <100 A have been removed, leaving 1019 current measurements, and a linear fit is made. As is clear, there is a well-defined linear relationship between the two currents with a high coefficient of determination ($r^2 = 0.982$). In this case there is only a small offset of 0.34 A in the fit to the TIM T5 LEM reported currents when the HVDC Earth return current was zero. This offset is not due to geomagnetic activity, which was low throughout this time period; rather, this is an example of the miss calibration of the LEM sensors mentioned in section 2.1. Linear fits of the LEM data allow us to remove the stray HVDC return current and also correct for calibration offsets, hence extracting high fidelity GIC values from the LEM measurements.

In order to do this, linear fits have been made across weekly data periods for all the LEM data, i.e., separately for each transformer. As GIC events will distort the relationship between total and stray HVDC Earth return current, we remove all time periods when the Eyrewell magnetic observatory *K* index are ≥5. We also remove periods with very low total HVDC Earth return currents (<100 A), as one mitigating strategy Transpower has employed is to decrease HVDC Earth return use during storms [*Marshall et al.*, 2012]. Figure 3b shows the long-term slope of the linear fit of the LEM data from TIM T5 from November 2001 to the end of December 2015. For the vast majority of the time the slope is essentially constant with a value of $-2.2 \times 10^{-3}$, such that 1000 A total HVDC Earth return current operation would lead to 2.2 A of stray

**Table 2.** Summary of the Operation of the HVDC Link Shown in Schematic in Figure 2

| Year | Percentage Time Total Earth Return HVDC > 100 A (%) | Average Yearly HVDC Total Earth Return Current (A) | Percentage Stray Current (%) |
|------|-----|------|-----|
| 2001 | 44.8 | 234 | 5.5 |
| 2002 | 52.1 | 201 | 5.7 |
| 2003 | 46.6 | 178 | 5.7 |
| 2004 | 53.9 | 277 | 5.6 |
| 2005 | 62.9 | 219 | 6.1 |
| 2006 | 69.4 | 235 | 5.9 |
| 2007 | 75.5 | 394 | 6.0 |
| 2008 | 99.7 | 841 | 6.0 |
| 2009 | 98.7 | 1057 | 7.6 |
| 2010 | 94.9 | 567 | 7.4 |
| 2011 | 94.1 | 565 | 7.5 |
| 2012 | 99.1 | 848 | 7.6 |
| 2013 | 64.4 | 553 | 6.0 |
| 2014 | 35.8 | 181 | 6.2 |
| 2015 | 42.4 | 161 | 6.5 |

current at TIM T5. We found that the short-lived deviations seen in the slope of Figure 3b are primarily caused by weekly time periods with only small amounts of current data, or in some rare cases where the linear fit is low quality. We remove those points by requiring that the coefficient of determination $r^2 > 0.5$ and also that there are at least 50 current measurements present throughout the week. When any of these two conditions were not met for a weekly interval, the slope was replaced with that of an accurate slope from an adjacent week. All such substitutions were manually checked to ensure that they were reasonable.

Figure 3c presents the long-term offset of the linear fit of the LEM data from TIM T5. As we have removed periods of geomagnetic activity, these offsets in the HVDC stray current reported during Earth return mode will represent miss calibration of the LEM sensors. Note that the offsets vary more than the slope of the linear fit, suggesting that they may play a very important role in the long-term data quality. In this sense we are fortunate for the presence of the HVDC stray current in our measurements, as they allow the removal of calibration offsets. Similar data sets collected in other parts of the world also contain quasi-constant offsets in the DC current (i.e., near constant nonzero currents outside of storm periods), which have to be corrected manually. While the offset varies more than the slope, it tends to remain essentially unchanged for significant periods (many months or more) before a value shift, as well as exhibiting some short-lived deviations. As in the case of the slope data plotted in Figure 3b, the short-lived deviations seen in Figure 3c were often due to poor correlations and number of samples and were treated in a similar way.

Using the slope, offset, and total HVDC return current, we can remove the predicted HVDC stray current from the TIM T5 data, producing a new "cleaned" data set which should be dominated by GIC. This is shown in Figure 3d for the year 2010. The panel includes both the original LEM currents and the GIC currents which have been determined by removing the influence of the HVDC operation. Note that 2010 was used as it was a comparatively quiet year geomagnetically, if not as quiet as 2009 (for example, see the discussion in *Rodger et al.* [2016]). Comparing this cleaned product to the original data shows how important correcting for HVDC operation is when considering the New Zealand DC data set. The original data (blue line) have a clear offset and also a larger range than the GIC data (magenta line).

The operation described above for TIM T5 has been repeated for all the LEM instrumented transformers to produce a "GIC data set" for all these locations. This operation has allowed us to estimate the total quantity of HVDC stray return current at each instrumented transformer, which is shown in Figure 4 for the year 2015. This figure describes the HVDC stray return current expected at each transformer for a 1000 A total HVDC Earth return current. The transformers are plotted with more northern locations at the top and more southern locations near the bottom. Red lines demarcate the values for the individual transformers in a single substation, for example, Invercargill has three instrumented transformers, while Manapouri has seven and South Dunedin one. The three green crosses in Figure 4 are for three transformers in Benmore which left the data set in September 2012, December 2012, and August 2013, respectively. These transformers were removed from service and hence will no longer have any HVDC stray return current present. Note that locations
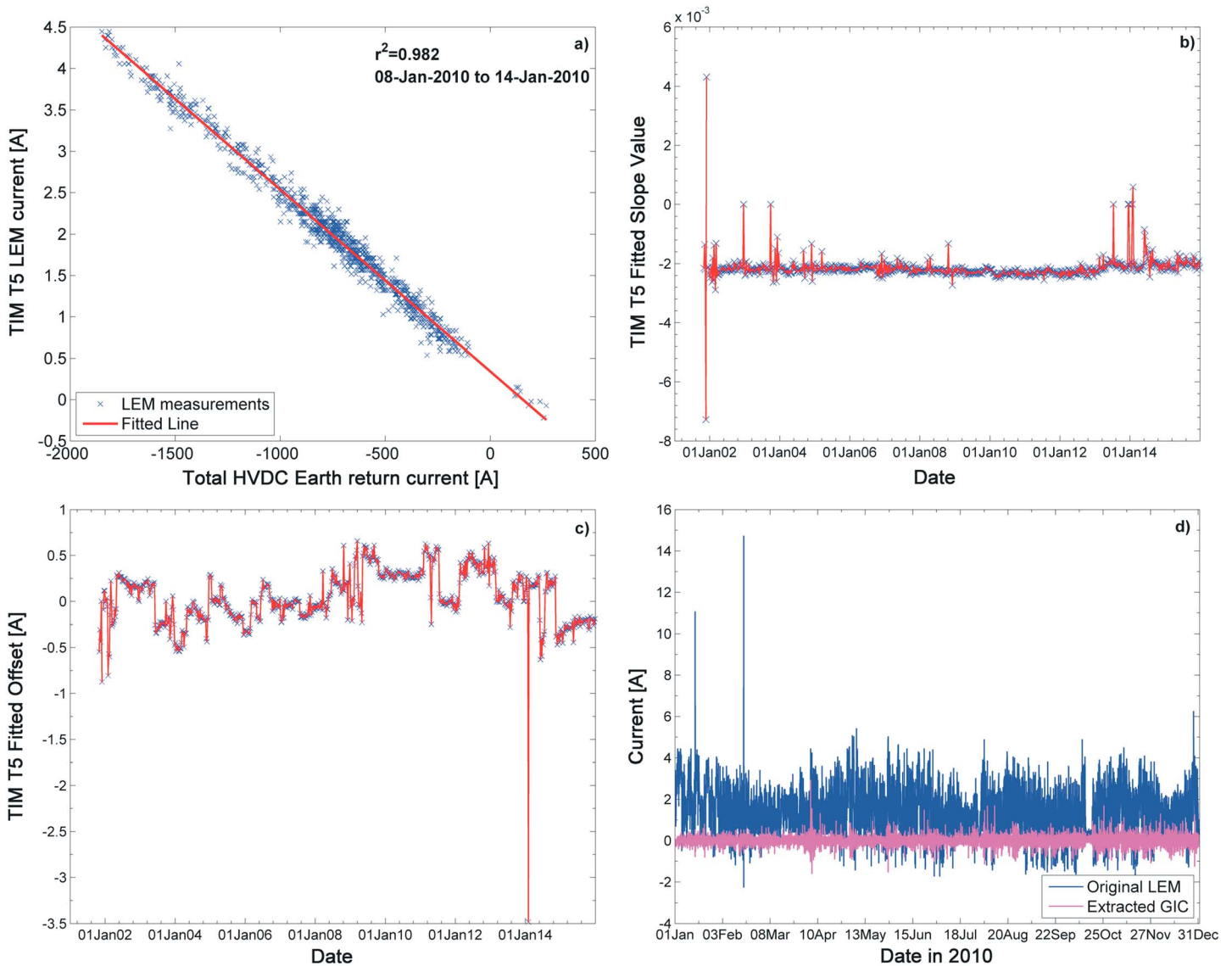
**Figure 3.** Images around the removal of stray HVDC Earth return currents from the LEM current measurements made at Timaru transformer T5 (TIM T5). (a) Relationship between the LEM-measured stray HVDC Earth return currents and the total HVDC Earth return current (blue crosses) for a 1 week example period, with a linear fit applied (red line), (b) variation of the slope of the linear fit to the stray and total HVDC currents across the entire time period, (c) variation in the offset of the linear fit across the entire time period, and (d) original LEM measurements (blue line) and the corrected GIC-only data (magenta) for 2010.

near Benmore tend to have higher values of HVDC stray return current, while those far from Benmore, for example, in the lower South island, tend to have lower values. The transformers at Benmore have only moderate levels of HVDC stray return current, despite being very close to the Bog Roy electrode. This is likely due to their unusual design features (including the installation of Neutral Earthing Resistors (NER) to mitigate the stray currents) which were specified in the original order, due to their operation near to the HVDC electrode.

Table 2 shows how the HVDC stray return currents summed across all the instrumented locations varies from year to year, as a percentage of the total HVDC Earth return current. The fraction of HVDC Earth return current which is measured as stray is typically 5.5–6.5% of the total current (i.e., ~94% of the current returns "directly"), with the maximum yearly range spanning 5.5–7.6%. On average across all years there is ~450 A of total HVDC Earth return current present, although this varies strongly from year to year (Table 2), which will lead to ~32 A of stray HVDC Earth return currents distributed into the South Island transformers.
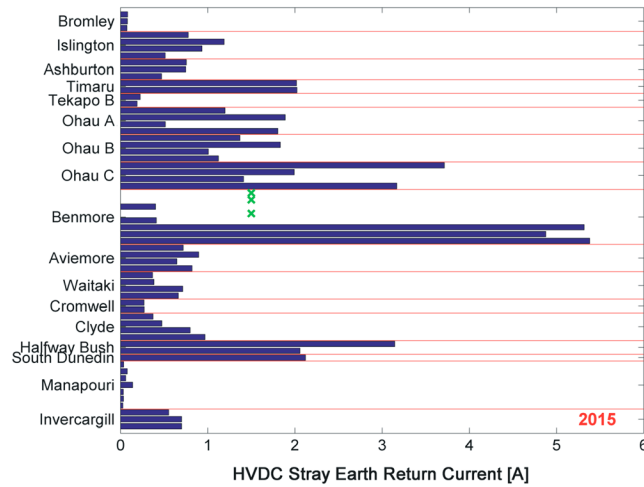
**Figure 4.** Magnitude of the stray HVDC Earth return currents which enter the transmission network through each of the LEM-monitored transformers for 2015, normalized to a total HVDC current of 1000 A. The red lines separate the individual substations inside of which multiple transformers may be monitored. The three green crosses are for transformers which had no LEM observations in 2015 due to being retired from operation.

During 2009–2012, which was during the restrictions on bipolar operation, Table 2 shows that the fraction of stray current increases to ~7.5% of the total current. This may reflect changes in the soil moisture at depths around the Te Hikowhenua and Bog Roy electrodes, due to the near-constant single wire Earth return mode operation. However, it might also reflect changes in the efficiency of the DC injection due to increased electrochemical erosion which occurs during this mode. The erosion rate at Bog Roy during the period of monopolar mode was 15 to 18 times higher than for bipolar operation [*Transpower*, 2013]. During this period more frequent maintenance was required at Bog Roy, and the buried electrode arms were progressively replaced [*Transpower*, 2013]. The Bog Roy electrode resistance will increase due to the higher corrosion, which increase the stray Earth return currents.

## 4. Storm of 6 November 2001: Network Response

*Marshall et al.* [2012] presented a detailed description of the Transpower South Island LEM observations during the geomagnetic storm of 6 November 2001, when the Halfway Bush T4 transformer (referred to as HWB T4) failed within 1 min of peak currents observed in the network, i.e., 14:52 NZDT [*Béland and Small*, 2004] which is 1:52 UT. The observations considered in the Marshall et al. paper will not be strongly impacted by stray HVDC return currents; single wire Earth return mode operation started from 22:00 NZDT (9 UT) on this day, which is well after the peak of the storm, and even then the maximum total HVDC Earth return current was only ~200 A. However, as stated earlier it is likely that offsets in the LEM measurements may be more important. In addition, the peak LEM currents reported in *Marshall et al.* [2012] are somewhat lower than we find in the GIC data set we describe here, which may be due to the data used by *Marshall et al.* [2012] being degraded to a lower time resolution (60 s).

Figure 5 presents the peak GIC current magnitudes seen in the instrumented transformers for the 6 November 2001 storm, in this case occurring in the minute of 1:52 UT (14:52 NZDT at this time of year). Figure 5 (right) uses a similar format to Figure 4 but color codes the GIC peak values for additional emphasis. The highest peak currents are ~33 A, seen at Islington transformer M6 (referred to as ISL M6), as reported by *Marshall et al.* [2012], but ~43% higher than was published in that work. For this storm there were also very strong currents (~31.5 A) at Tekapo B and Ohau A, near the centre of the South Island. In contrast, the GICs measured at Benmore and Aviemore, just ~70 km away, were only a few amps, as is shown in Figure 5 (left). These large differences in peak GIC magnitude over small distances indicate the need for theoretical modeling to predict and understand the detailed impact of GIC in New Zealand during storms. It is likely that they are caused by a combination of network configuration, transformer design, and varying ground structure. For example, Figure 5 shows that Benmore and Aviemore have NER installed, while Tekapo B and Ohau A do not. The large variability seen in Figure 5 is consistent with recent modeling results for the Irish power grid [*Blake et al.*, 2016], where a constant 1 V/km geoelectric field produced large variations in GIC current throughout the network due to network configuration and differing ground conductivity.
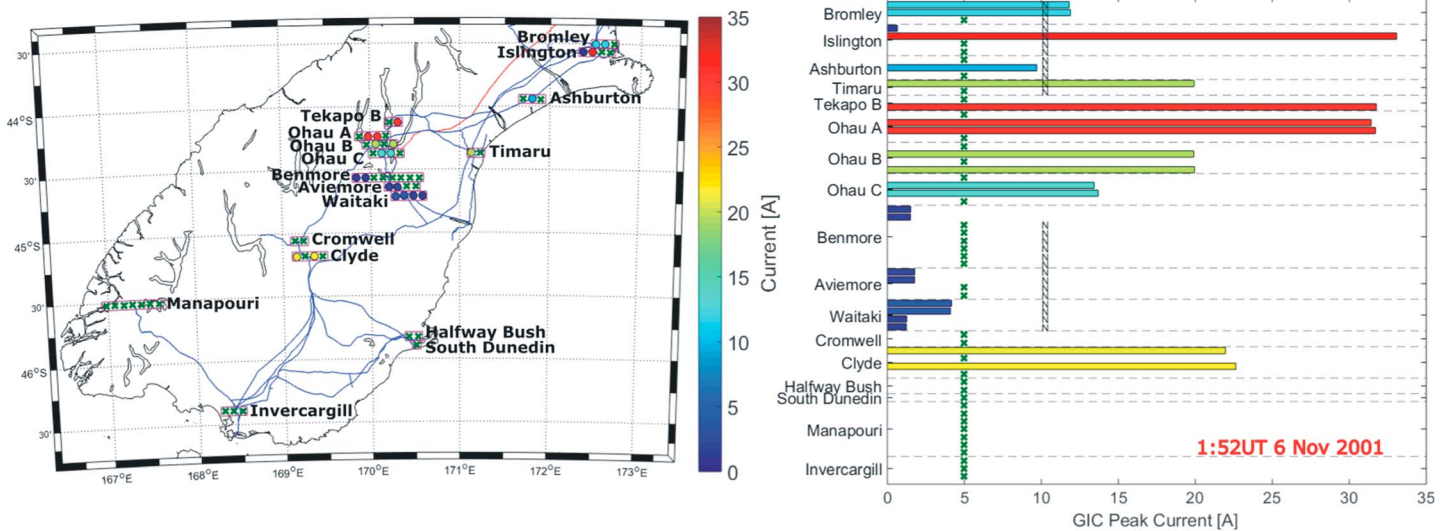
**Figure 5.** Magnitudes of the peak GIC observed at 1:52 UT during the geomagnetic storm of 6 November 2001. (left) A geographical map including the transmission lines (blue) and the path of the HVDC link (red). Each box represents a substation (as named), with colored circles for the individual transformer measurements. (right) A similar format to Figure 4. Green crosses in both panels mark transformers which were not LEM monitored at this time. The letter "N" in Figure 5 (right) indicates transformers with Neutral Earthing Resistors.

## 5. Comparison With Geomagnetic Driver: Case Studies

### 5.1. Case Study—6 November 2001

Large GICs are usually closely associated with geomagnetic field disturbances that have a high rate of change ($dB/dt$) and, in particular, the rate of change of the magnetic component in the horizontal direction ($dB_H/dt$, also represented by $H'$) [*Mäakinen*, 1993; *Viljanen*, 1998; *Bolduc et al.*, 1998]. *Thomson et al.* [2011] examined 30 years of 1 min resolution digital data from 28 European observatories and found that peak $H'$ increased with magnetic latitude, with a distinct maximum in extreme levels between ~53 and 62° latitude. The primary argument for considering the time derivative of the magnetic field is that it is a good indicator of the expected magnitude of the geomagnetically induced electric field on the Earth's surface [*Cagniard*, 1953], which is the primary driver of GICs [e.g., *Viljanen et al.*, 2001]. Despite this expectation, a study carried out using observations from a power grid in Memanbetsu, Hokkaido (Japan), showed that GICs were more strongly associated with the deviation of the $Y$ and $Z$ magnetic field components, not the horizontal rate of change [*Watari et al.*, 2009a, 2009b]. We examine this suggestion in detail below and follow their approach by looking at the correlation coefficients between the GIC and the magnetic field components.

As a starting point we undertake a case study around the 6 November 2001 geomagnetic storm, as significant analysis of this event has already been published in the literature. This storm has been described in detail by *Marshall et al.* [2012], and thus, we limit ourselves to a few overview comments. The storm peaked with a global $Kp = 9-$ with the local Eyrewell K index being $K = 8$. The storm started with a sudden commencement 01:52 UT; from 0 to 3 UT the Eyrewell-observed $H$ component of the magnetic field changed from 21,093 nT to a maximum of 21,594 nT (a range of 501 nT). This is shown in Figure 6 (top), where the right-hand axis presents the variation in the $H$ component of the magnetic field measured at Eyrewell around the time of the sudden commencement. In contrast, the peak in the $H'$ component was measured as 191 nT/min, also occurring at 01:52 UT. This is shown in Figure 6 (bottom), again through the dashed line (in this case red colored) referring to the right-hand axis.

We initially focus on the correlation between magnetic field variations and the GIC measured at the Islington transformer M6 (referred to as ISL M6), as this transformer had the largest GIC observed during this storm. The 1 min averaged GIC observations are shown in Figure 6 (top and bottom), through the solid line referring to the left-hand axis, peaking at a value of 20.6 A. Figure 6 (top) contrasts the time variation of the Eyrewell $H$ component of the magnetic field with the ISL M6 measured GIC, both with 1 min time resolution. The Pearson correlation coefficient between the GIC and the $H$ component amplitude is 0.61. We follow the
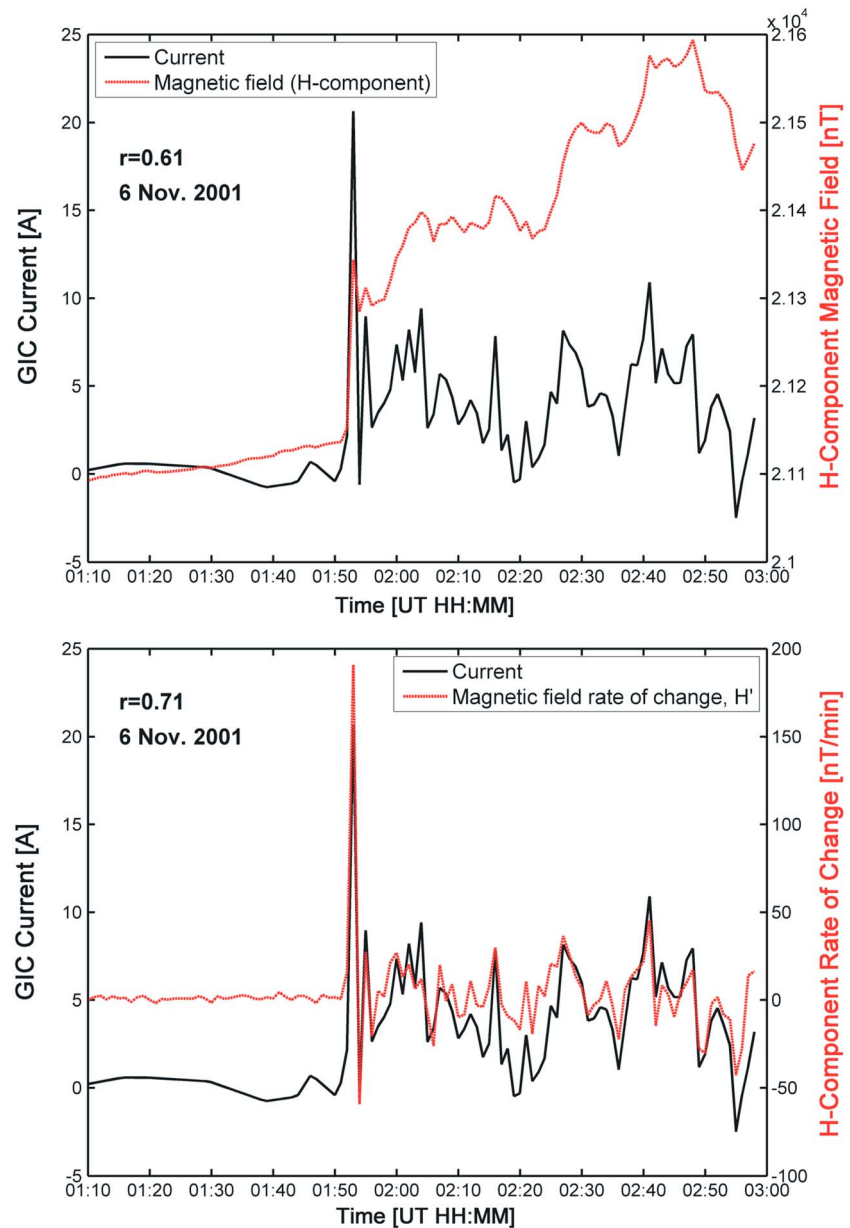
**Figure 6.** Comparison between the Eyrewell (EYR) measured magnetic field and the GIC observed at Islington transformer M6 (ISL M6) on 6 November 2001, both with 1 min time resolution. (top) The variation of the amplitude of the *H*-component of the EYR magnetic field with the ISL M6 GIC. (bottom) The variation of the rate of change of the *H*-component (i.e., *H'*) with the ISL M6 GIC. The *r* values reported are the Pearson correlation coefficients.

common practice of examining the *p* value to test if the Pearson correlation coefficient is statistically significant (for an overview on *p* values see a statistics textbook [e.g., *Martin*, 2012] or overview article [e.g., *Rodgers and Nicewander*, 1988; *Du Prel et al.*, 2009]). If the *p* value is small ($p < 0.05$), it is generally assumed that the null hypothesis may be rejected and the correlation assumed to be "statistically significant". In this case the *p* value is $2.8 \times 10^{-12}$, indicating a clearly significant relationship.

Figure 6 (bottom) contrasts the time variation of the rate of change of the *H* component (i.e., *H'*) with the ISL M6 measured GIC. In this case the linear correlation is higher (0.71) and the agreement "by eye" is clearer, as expected for a larger correlation coefficient, as it implies a stronger relationship. This is also consistent with the very small *p* value, which is only $3.6 \times 10^{-18}$.

**Table 3.** Examination of the Varying Number of Transformers Where the Observed GIC Correlates Best With the Given Magnetic Field Component, Amplitude or Rate of Change[a]

| 6 Nov 2001 | H | H′ | X | X′ | Y | Y′ | Z | Z′ | F | F′ |
|---|---|---|---|---|---|---|---|---|---|---|
| All transformers | 4 | 8 | 4 | 2 | 6 | 0 | 0 | 0 | 3 | 4 |
| Mean $r$ | 0.80 | 0.76 | 0.80 | 0.71 | 0.77 | - | - | - | 0.72 | 0.71 |
| Median $r$ | 0.80 | 0.76 | 0.82 | 0.71 | 0.78 | - | - | - | 0.70 | 0.74 |
| Mean GIC [\|A\|] | 1.4 | 15.2 | 0.5 | 7.2 | 4.2 | - | - | - | 0.8 | 10.2 |
| non-NER transformers | 1 | 7 | 0 | 0 | 3 | 0 | 0 | 0 | 1 | 2 |
| Mean $r$ | 0.71 | 0.77 | - | - | 0.77 | - | - | - | 0.83 | 0.76 |
| Median $r$ | 0.71 | 0.76 | - | - | 0.78 | - | - | - | 0.83 | 0.76 |
| Mean GIC [\|A\|] | 0.9 | 14.4 | - | - | 5.1 | - | - | - | 1.1 | 13.5 |

[a]The upper section of the table is for all 31 transformers which were monitored during this event; the lower section of the table is for the 14 non-Neutral Earthing Resistor (NER) transformers only. This table presents parameters across the time period 01:10–3:00 UT on 6 November 2001 and includes a total of 31 distinct transformers. The $r$ values reported are the Pearson correlation coefficients, and in all cases we only include Pearson correlation coefficients when the $p$ value is smaller than 0.05.

Similar comparisons have been made with all of the magnetic field components and also the rates of change of these components. The Pearson correlation coefficients with the ISL M6 GIC and different magnetic field components are 0.607 ($H$), 0.713 ($H′$), 0.594 ($X$), 0.704 ($X′$), 0.653 ($Y$), 0.577 ($Y′$), −0.268 ($Z$), −0.555 ($Z′$), 0.473 ($F$), and 0.691 ($F′$). All have $p$ values <0.05. Note that $H$, $X$, and $Y$ (and their time derivatives) are not statistically independent of one another, given that they are directly linked components. We provide all of these correlation coefficients to allow contrasts between earlier studies who have considered $X$, $Y$, and $Z$ components [e.g., *Viljanen et al.*, 2006; *Watari et al.*, 2009a, 2009b] or the horizontal field component $H$ [e.g., *Viljanen et al.*, 2001; *Thomson et al.*, 2011].

Clearly, in most cases the highest correlation coefficients for the ISL M6 GIC tend to be found in the rate of change of the magnetic field components, with the highest for $H′$. This is consistent with multiple previous studies but not with *Watari et al.* [2009a]. One possible suggestion put forward by *Watari et al.* [2009a] was that their measurements might be influenced by the coastal effect. Islington (ISL) is located ~15 km from the sea, whereas Memanbetsu is ~13 km from the sea, and therefore, the coastal effect does not appear to be responsible for the *Watari et al.* [2009a] finding. Another suggestion was that the Memanbetsu GIC observations might be different due to their geomagnetic latitude. As these were made ~10° equatorward of any of the South Island GIC observations we cannot discount this.

We now consider the Pearson correlations for all 31 transformers for which there were GIC observations during this storm. The correlations were calculated from 01:10 to 03:00 UT, which is the time period shown in Figure 6. We only consider Pearson correlation coefficients where the associated $p$ value is smaller than 0.05. The results are presented in the upper part of Table 3. Note that 31 is larger than the number of transformers with peak currents shown in Figure 5, because 8 additional transformers have no GIC measurements at 1:52 UT but were operating throughout most of the time window such that correlations can be examined. Overall, the largest number of transformers shows the best correlation with the $H′$ component, in this case, 8. In contrast, the amplitude of $H$ has the highest correlation at four transformers, but the amplitude of the $Y$ component has the highest correlation coefficient at six transformers. The mean and median linear correlation coefficients for the transformers with the highest correlation with that component are also shown in this table. From the table, it initially appears that the highest Pearson correlation coefficients (~0.8) are seen for four transformers with the amplitude of the $H$ component, four transformers with the amplitude of the $X$ component, and six transformers with the amplitude of the $Y$ component. This seems unexpected, as it disagrees with our earlier analysis of the ISL M6 data and the findings of most, if not all, of the literature. The likely explanation for this can be found in the lowest row of this table, which shows the mean GIC magnitude for the transformers in question. In the case of transformers which show the highest correlation with the rate of change of the magnetic component (i.e., $H′$, $X′$, and $F′$), the mean currents are considerably higher than at the transformers which show the highest correlation with the amplitudes of magnetic field components (i.e., $H$, $X$, $Y$, and $F$). This is particularly clear when considering the eight transformers which correlate best with $H′$. These transformers have a mean GIC magnitude of 15.2 A and typical correlation coefficients of ~0.76. This should be contrasted with the four transformers that have the highest correlation coefficients with the $X$
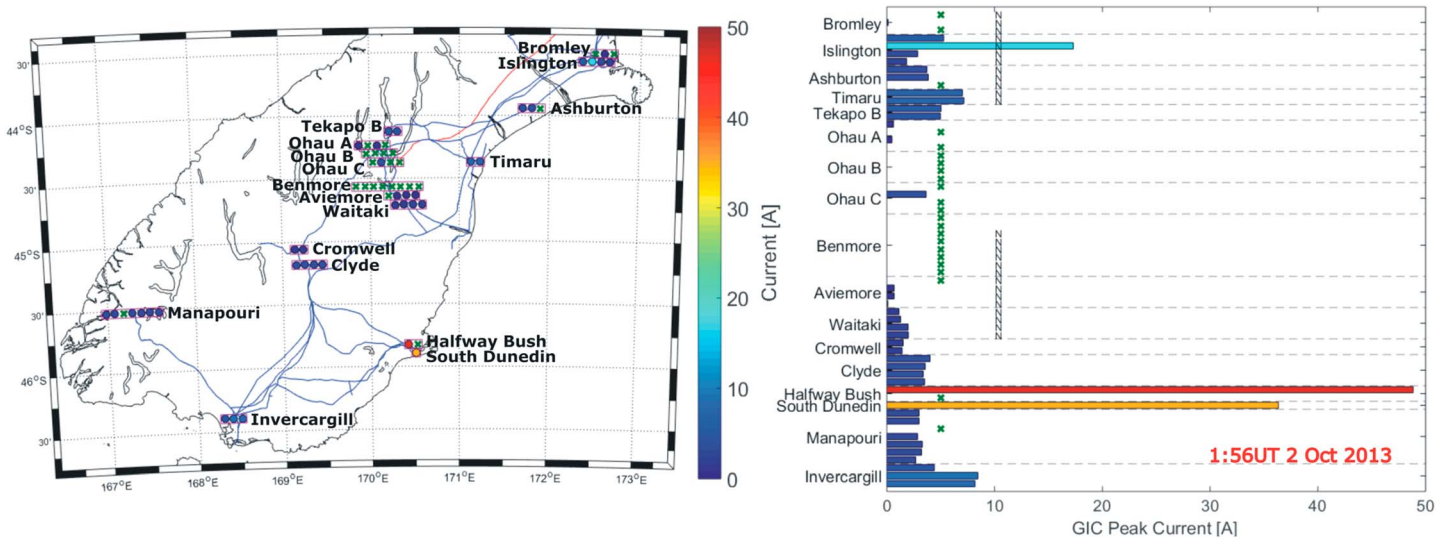
**Figure 7.** As in Figure 5 but showing the observations for the peak GIC magnitudes observed at 1:56 UT during the storm on 2 October 2013.

component. The four transformers have a mean GIC magnitude of only 0.5 A. We suggest that smaller induced current values will be more affected by noise, occasionally masking the correlation with the physical driver (i.e., $H'$).

We consider this suggestion by undertaking the same analysis on the 14 transformers which were not fitted with a NER for which there are data for this time period. NER have been fitted to many of the monitored transformers to decrease the magnitude of the stray HVDC return current and will likely decrease the magnitude of the GIC at that transformer (see the discussion in *Pirjola* [2008]). Figure 5 (right) indicates which transformers have NER installed, and the corresponding analysis of correlation coefficients for this storm period is shown in the lower part of Table 3. Again, the largest number of transformers shows the best correlation with the $H'$ component, in this case, 7. Only one transformer showed the highest correlation with $H$, and none with $X$, or $Z$ components. Nonetheless, it is worth noting that three transformers have the best correlation with $Y$ component with reasonable Pearson correlation coefficients (~0.8) and mean GIC (5.1 A).

### 5.2. Case Study—2 October 2013

We also undertake similar analysis of a more recent event which contained the largest GIC current magnitude measurement throughout the available data set, when a larger number of LEM systems were installed, and hence, more GIC-monitored transformers are available to test. We focus on the geomagnetic storm from 0 to 6 UT on 2 October 2013, during which $Kp$ reached a maximum value of 8−, the local (to New Zealand) Eyrewell $K$ index peaked at 6 (from 3 to 6 UT), and we have GIC observations from 49 distinct locations (the remaining 7 transformers have no measurements available in that 6 h period). Across this time period the HVDC link was continuously operating in single wire Earth return mode, with currents ranging from ~100 A up to values as high as ~1020 A. GIC modeling and observations from a single location in Brazil during this storm have appeared in the literature [*Barbosa et al.*, 2015].

The storm resulted in two distinct times of geomagnetic variations observed at Eyrewell. The first period began with a sudden commencement at 01:56 UT at which time there was a large $H$ component variation and rate of change (117 nT and 86 nT/min, respectively). This was followed by a further pulse of strong variability at ~04:34 UT which was associated with a larger horizontal $H$ component variation of 177 nT but a smaller $H'$ measurement of 53 nT/min.

Figure 7 shows the magnitudes of the peak GIC observed in the minute of 1:56 UT of this storm, in the same format as Figure 5. The largest GIC values were seen during the initial sudden commencement, with 19.1 A recorded at ISL M6, and 48.9 A at HWB T4. Figure 8 (top) shows the comparison between the ISL M6 observed GIC and the amplitude of the EYR-measured $H$ component, in the same format as Figure 6. The Pearson correlation coefficient ($r$) for this data set is −0.31 ($p = 1.4 \times 10^{-9}$). In contrast, Figure 8 (bottom) shows a comparison between the ISL M6 GIC and the EYR $H'$, which has an $r$ value of −0.95 ($p = 6.4 \times 10^{-185}$) and a much
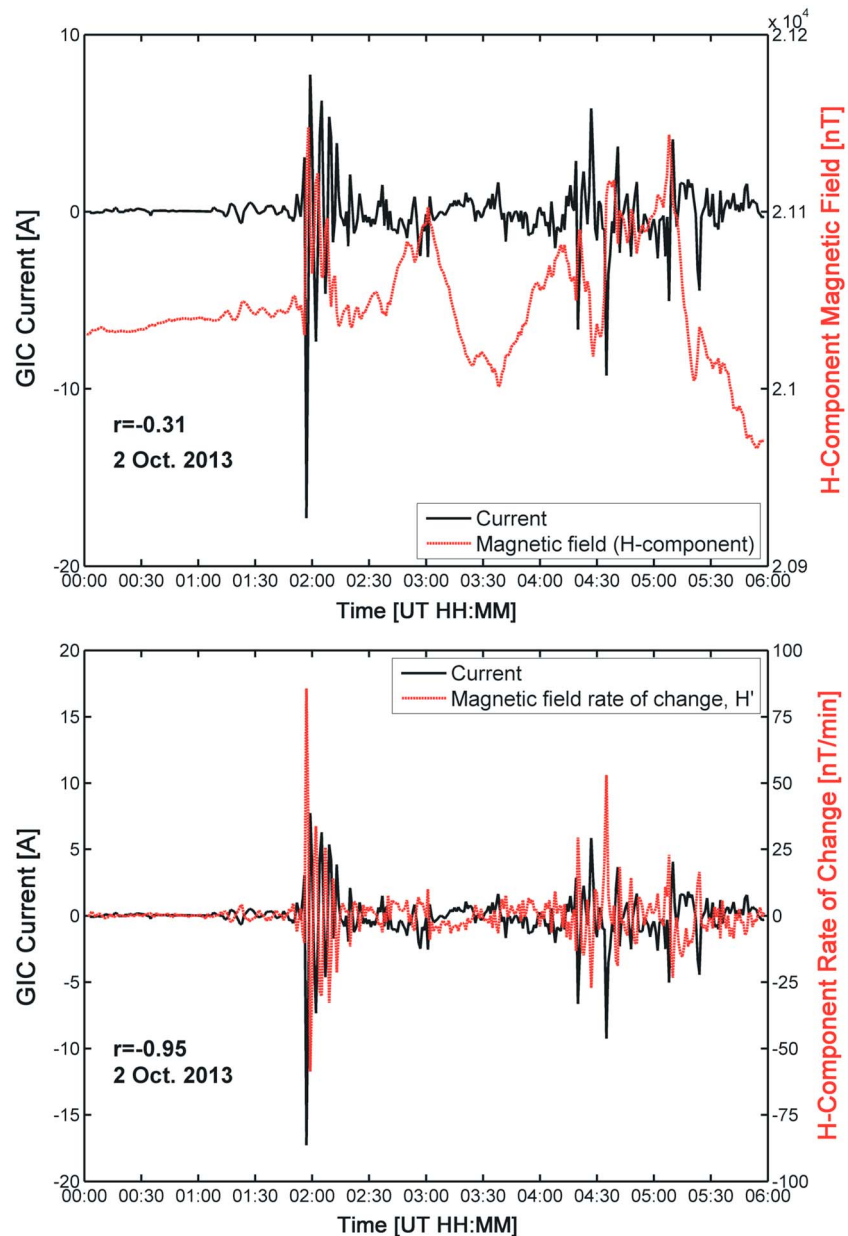
**Figure 8.** As Figure 6 but showing the observations for a storm on 2 October 2013.

closer by eye agreement. The Pearson correlation coefficients with the ISL M6 GIC and different magnetic field components during this storm are −0.31 (H), −0.95 (H′), −0.28 (X), −0.94 (X′), −0.29 (Y), −0.70 (Y′), 0.09 (Z), 0.74 (Z′), −0.21 (F), and −0.89 (F′). Most of the correlation coefficients are statistically significant, expect for the correlation with the Z component where $p = 0.09$. Note that the majority of the correlation coefficients are negative in this case. The likely reason for this is that the data in the Transpower archive system have been inverted at some point; the primary reason for the LEM sensors is to monitor the magnitude of the stray HVDC Earth return currents, and there is much less focus on the direction of the current from Transpower's perspective. When considering the typical response across the entire data set (below), we use the magnitude of the GIC.

The upper section of Table 4 shows a summary of the highest correlations between GIC and magnetic field components for 47 transformers from on 2 October 2013, in the same format as Table 3. As in the previous case the correlations were examined from 00 to 06 UT on this day, the time period plotted in Figure 8. While there were 49 transformers providing GIC observations in this time period, two fail the $p$ value test

**Table 4.** As Table 3 but for the Time Period 00–06 UT on 2 October 2013, Including a Total of 47 Distinct Transformers (Upper Section) and 26 Distinct Non-NER Transformers (Lower Section)

| 2 Oct 2013 | H | H′ | X | X′ | Y | Y′ | Z | Z′ | F | F′ |
|---|---|---|---|---|---|---|---|---|---|---|
| All transformers | 7 | 19 | 5 | 7 | 1 | 0 | 5 | 1 | 0 | 2 |
| Mean r | 0.58 | 0.74 | 0.61 | 0.63 | 0.33 | - | 0.51 | 0.73 | - | 0.56 |
| Median r | 0.61 | 0.75 | 0.75 | 0.72 | 0.33 | - | 0.55 | 0.73 | - | 0.56 |
| Mean GIC [\|A\|] | 1.8 | 5.8 | 4.3 | 9.0 | 0.03 | - | 1.2 | 0.1 | - | 2.2 |
| non-NER transformers | 2 | 10 | 3 | 6 | 1 | 0 | 1 | 1 | 0 | 2 |
| Mean r | 0.46 | 0.73 | 0.75 | 0.67 | 0.33 | - | 0.52 | 0.73 | - | 0.56 |
| Median r | 0.46 | 0.76 | 0.75 | 0.72 | 0.33 | - | 0.52 | 0.73 | - | 0.56 |
| Mean GIC [\|A\|] | 0.7 | 6.5 | 7.0 | 10.4 | 0.03 | - | 3.7 | 0.1 | - | 2.2 |

($p < 0.05$) and have been excluded from the analysis presented in Table 4. Clearly, the majority of the transformers (19 out of 47) correlate best with the rate of change of the horizontal field, and to a lesser extent X′ (7 out of 47), with fairly strong currents (>5 A) and high correlation coefficients. There are, however, a smaller set of transformers (5 out of 47) which have reasonable GIC magnitudes (~4.3 A), fairly high Pearson correlation coefficients, that correlate best with the amplitude of the X component. If the New Zealand observations were limited to just one of these locations, as was the case of the single site in Hokkaido considered by *Watari et al.* [2009a], we might concur with their conclusions, at least for this storm. However, one might expect that local ground conductivity near these transformers could influence the relationship between the magnetic and electric fields [e.g., *Trichtchenko and Boteler*, 2006]. As impedance relates the magnetic field to electric field in the frequency domain, a ground structure with relatively low conductivity at deep layers would cause low-frequency components of the driving magnetic field to have more influence than high-frequency components. Such an effect could cause an apparent correlation with the amplitude of H rather than the rate of change of this component. While this is possible, one would expect the deep conductivity structure to remain unchanged, such that one would find that some transformers consistently correlated with the amplitude of H in many geomagnetic storm events. That is not the case in our examination of the New Zealand data, and specially, there is no agreement between the two case studies in that we do not find that any the transformers consistently favor the X or H component amplitude over the rate of change.

The lower section of Table 4 presents the analysis for non-NER transformers. Again, the majority of the transformers (10 out of 26) correlate best with the rate of change of the horizontal field or X′ (6 out of 26), with fairly strong currents (>6.5 A) and high correlation coefficients. There remains a set of three transformers which have reasonable GIC magnitudes (~7.0 A), fairly high Pearson correlation coefficients, and correlate best with the amplitude of the X component. These three transformers are all located in the Invercargill substation, and were not providing GIC observations until 2012, thus were not included in the analysis in section 5.1. We have specifically checked to see if these transformers tend to correlated with the X component in other geomagnetic storms, but find this is not the case. In the vast majority of cases, the correlation is best with the H′ component.

## 6. Comparison With Geomagnetic Driver: Long Term

In section 5 we looked at the correlation between observed GIC and geomagnetic drivers in two case study storms. We now attempt to re-examine the correlation for the entire data set. In order to do this, we identify hourly periods which are "disturbed" and worthy of detailed consideration. We do this by setting the requirements that either observed GIC are high or there are large magnetic field variations. Generally, the most responsive LEM-instrumented transformers are ISL M6, HWB T4, and also the number 6 transformer at Halfway Bush (HWB T6) plus South Dunedin transformer number 2 (SDN T2). We identify 151-hourly periods across the entire data set by requiring that one or more of the following requirements are met:

1. Peak 1 min averaged GIC magnitude is ≥10 A at anyone of ISL M6, HWB T4 HWB T6, or SDN T2, for any time during that hour.
2. The peak-to-peak variation in the EYR H is ≥200 nT (i.e., the difference between the maximum and minimum values in the hour exceeds this threshold).
3. The peak 1 min resolution value of EYR |H′| is ≥50 nT/min.

**Table 5.** Summary of Correlations Between the Hourly Time Varying GIC at ISL M6 and Components of the EYR-Observed Magnetic Field for 151-Hourly Periods Identified Through the Criteria in Section 6[a]

| Component | Number Periods Good Correlation | Percentage of Total Periods |
|---|---|---|
| $H$ | 6 | 4.0% |
| $H'$ | 98 | 64.9% |
| $X$ | 11 | 7.3% |
| $X'$ | 52 | 34.4% |
| $Y$ | 9 | 6.0% |
| $Y'$ | 19 | 12.6% |
| $Z$ | 12 | 7.9% |
| $Z'$ | 13 | 8.6% |
| $F$ | 9 | 6.0% |
| $F'$ | 71 | 47.0% |

[a]A good Pearson correlation coefficient is required by setting $r \geq 0.8$ and $p < 0.05$. The percentage refers to the percentage relative to the 151 total periods.

### 6.1. Islington Transformer M6

As before, we start by considering ISL M6 as it has the longest continuous data set and has observations for all the 151 h considered. We then require that there is a "good" statistically significant Pearson correlation coefficient between the magnetic field component and the GIC time variation, i.e., $r \geq 0.8$ and $p < 0.05$. The number of hourly periods for which this holds for ISL M6 is shown in Table 5. Of the 151 time periods 98 (~65%) have good correlations with $H'$, to be compared with only 6 periods (4%) having good correlations with $H$. Clearly, there are more high correlation periods for the rates of change of the geomagnetic field rather than its amplitude, with by far the best agreements being with $H'$, consistent with most, if not all, of the previous literature.

### 6.2. All South Island LEM-Monitored Transformers

Following the same approach, we test the result for all transformers. Based on our findings around small-current observations which are more likely to be impacted by noise, we consider only hourly periods for which the peak GIC magnitude is $\geq 5$ A. This value was determined by checking the peak hourly GIC magnitude for ISL M6 for the International Quiet Days, which provided the 10 geomagnetically quietest days for each month, generating 1800 quiet days from the start of 2001 to the end of 2015. This was used to determine ISL M6 peak GIC magnitudes occurring on the quiet days, producing 38,371 values with 1 h resolution. Only 13 of these values were $>5$ A, suggesting that it is a reasonable threshold for "significant" GIC.

The limitations described above leave us with 36 transformers, as 25 never report currents this high, and the maximum number of time periods decreases to 83 (note that the number of time periods available varies for each transformer). For each LEM-monitored transformer, we examine the percentage of available periods where there is a good statistically significant Pearson correlation coefficient, i.e., $r \geq 0.8$ and $p < 0.05$. We then find which component has the maximum number of good correlation periods. A sum is taken of these across all 36 transformers to determine the number of transformers which have high-quality correlations for the disturbed hourly periods. If a transformer has equally good correlation percentages between components, the weighting is shared equally. As an example, HWB T6, for which data collection has only recently started, has only 14 disturbed hourly time periods. The 57.1% show good correlation with $H'$, 28.6% with $X'$, 28.6% with $F'$ with no other components having good correlations for more than two 1 h time periods. Therefore, HWB T6 will be included as one transformer showing the best high-quality correlation with $H'$. Table 6 shows the number and percentage of transformers which have the best high-quality correlations with each component. Note that six transformers had no components for which there was a good correlation but also suffered from a lack of observations ($\leq 3$ h periods).

Through this operation we find that the weighted number of transformers which have the best high-quality correlation between GIC and $H'$ is 17.2 (47.8%), with the next highest two values being $F'$ (3.5 weighted transformers and 9.7%) and $X'$ (3.1 and 8.7%). Once again, the rate of change of the horizontal magnetic field component has the strongest correlation with the observed GIC, confirming the generally reported conclusions that $H'$ is the primary driver of GIC.

**Table 6.** Summary of the Weighted Number of Transformers With the Best Correlation Between the Hourly Time Varying GIC and Components of the EYR-Observed Magnetic Field[a]

| Component | Number Transformers Good Correlation | Percentage of Total Transformers |
|---|---|---|
| H | 0 | 0.0% |
| H′ | 17.2 | 47.8% |
| X | 1.8 | 4.9% |
| X′ | 3.1 | 8.7% |
| Y | 2.1 | 5.9% |
| Y′ | 0 | 0.0% |
| Z | 1.1 | 2.9% |
| Z′ | 0.1 | 0.4% |
| F | 1.1 | 2.9% |
| F′ | 3.5 | 9.7% |
| none | 6 | 16.7 |

[a]A good Pearson correlation coefficient is required, $r \geq 0.8$ and $p < 0.05$. The percentage refers to the percentage of the 36 transformers across the South Island which meets the criteria described in section 6.2.

## 7. Summary

Transpower New Zealand Limited has measured DC currents at transformer neutrals in the New Zealand electrical network at multiple South Island locations. The primary reason for the DC current observations is to monitor stray currents entering the AC transmission network when the HVDC system linking the North and South Islands operates in Earth return mode. Near-continuous archived DC current data exist since 2001, starting with 12 different substations and expanding from 2012 to include 17 substations. The original focus of the measurements was primarily upon the impact of the HVDC link, while the additional substations monitored from 2012 onward were added due to Space Weather concerns, specifically around GIC. Across the time period 2001–2015 DC measurements were undertaken at a total of 61 distinct transformers (up to 58 transformers at any given time). The majority of the time the DC measurements are dominated by stray currents during HVDC Earth return operation and also suffer from nonzero calibration. However, by correcting for the stray currents during single wire Earth return HVDC mode, we can both remove the stray currents and correct for the calibration problems. This leads to an unusually dense set of near-continuous GIC observations at multiple substations spanning almost 14 years.

In our study we have described and demonstrated the procedure by which the DC measurements may be corrected. As there are many HVDC systems across the world, some of which use Earth return; the approach may be important for other Space Weather researchers. We also provide information on the level of stray current during Earth return HVDC mode and its variation across the South Island network.

We examine in detail the peak GIC magnitude reported across the South Island for the geomagnetic storms of 6 November 2001 and 2 October 2013. A transformer suffered permanent failure in Halfway Bush (Dunedin) during the 6 November 2001 storm, and the maximum GIC values ever recorded in Dunedin (to date) were observed on 2 October 2013 by the newly installed DC monitors. Peak GIC magnitudes are ~30 A (6 November 2001) and ~50 A (2 October 2013), comparatively large values by the standards of nonextreme storms reported in the literature.

There is some disagreement in the literature concerning the primary drivers of GIC. While most studies to date have concluded that GIC are best correlated with the rate of change horizontal component of the time-varying geomagnetic field (i.e., H′), *Watari et al.* [2009a, 2009b] reported that GIC measured at their midlatitude near-coastal location in northern Japan were best correlated with the amplitude of the east (Y) or vertical (Z) field components. We have examined this in some detail. For most time periods and locations we find that the rate of change of the horizontal geomagnetic field (H′) correlates best with the observed GIC. For high-quality statistically significant Pearson correlation coefficients ($r \geq 0.8$ and $p < 0.05$) this is particularly clear when GIC magnitude is sufficiently high to allow clear comparisons. While the horizontal geomagnetic field (H) component is derived from the north (X) and east (Y) components, the significant difference between our study and the *Watari et al.* [2009a] study is the finding that the rate of change of the magnetic field components tends to have much higher correlation coefficients with GIC than the correlation found with the component amplitudes. *Watari et al.* [2009a] suggested that the coastal effect might explain the

difference between their findings and that more commonly found. We specifically examined a long-lasting data set collected a similar distance from the coast and could not confirm their suggestion.

In one case study we found that there was a small set of transformers (5 out of 47) which have small but clear GIC magnitudes (~4.3 A), fairly good correlation coefficients, and correlate best with the amplitude of the *X* component of the geomagnetic field. If the New Zealand observations were limited to just one of these locations, as was the case of the single site in Hokkaido considered by *Watari et al.* [2009a, 2009b], we might concur with their conclusions, at least for that storm (2 October 2013). Thus, while we conclude that generally *H′* provides the best correlations, for some locations and reasonably small GIC magnitudes during some storms might appear to correlate well with the change in the amplitude and not the rate of change.

We suggest that the large New Zealand GIC data set will provide additional useful insights into Space Weather. The current study is a first step to understanding this data set. Our research group is now undertaking more research and also constructing a model to predict GIC in New Zealand to be validated by the experimental observations described in a detailed way here. The two storms presented in detail in the current study show quite a different spatial response during the storm peak (i.e., peak GIC occurring in different locations), emphasizing the need for detailed modeling.

## References

Ardelean, M., and P. Minnebo (2015), HVDC submarine power cables in the world, JRC technical reports, Publications Office of the European Union, doi:10.2790/023689.

Barbosa, C., L. Alves, R. Caraballo, G. A. Hartmann, A. R. R. Papa, and R. J. Pirjola (2015), Analysis of geomagnetically induced currents at a low-latitude region over the solar cycles 23 and 24: Comparison between measurements and calculations, *J. Space Weather Space Clim.*, *5*, 9.

Beck, C. (2013), The international E-Pro™ report: International electric grid protection, Electric Infrastructure Security Council, EIS Council, Washington, D. C.

Béland, J., and K. Small (2004), Space Weather effects on power transmission systems: The cases of Hydro-Québec and Transpower New Zealand Ltd, in *Effects of Space Weather on Technological Infrastructure*, edited by I. A. Daglis, pp. 287–299, Kluwer Acad., Netherlands.

Blake, S. P., P. T. Gallagher, J. McCauley, A. G. Jones, C. Hogg, J. Campanya, C. Beggan, A. W. P. Thomson, G. S. Kelly, and D. Bell (2016), Geomagnetically induced currents in the Irish power network during geomagnetic storms, *Space Weather*, *14*, 1136–1154, doi:10.1002/2016SW001534.

Bolduc, L. (2002), GIC observations and studies in the Hydro-Québec power system, *J. Atmos. Sol. Terr. Phys.*, *64*, 1793–1802.

Bolduc, L., P. Langlois, D. Boteler, and R. Pirjola (1998), A study of geoelectromagnetic disturbances in Quebec, 1. General results, *IEEE Trans. Power Delivery*, *13*, 1251–1256.

Carter, B. A., E. Yizengaw, R. Pradipta, A. J. Halford, R. Norman, and K. Zhang (2015), Interplanetary shocks and the resulting geomagnetically induced currents at the equator, *Geophys. Res. Lett.*, *42*, 6554–6559, doi:10.1002/2015GL065060.

Carter, B. A., E. Yizengaw, R. Pradipta, J. M. Weygand, M. Piersanti, A. Pulkkinen, M. B. Moldwin, R. Norman, and K. Zhang (2016), Geomagnetically induced currents around the world during the 17 March 2015 storm, *J. Geophys. Res. Space Physics*, *121*, 10,496–10,507, doi:10.1002/2016JA023344.

Cagniard, L. (1953), Basic theory of the magnetotelluric method of geophysical prospecting, *Geophysics*, *18*, 605–635, doi:10.1190/1.1437915.

Dalzell, M. (2011), DC currents in the New Zealand AC power system, paper presented at conference and exhibition, *Electr. Eng. Assoc.*, Auckland, N. Z., 23–24 June.

Dayton, L. (1989), Solar storms halt stock market as computers crash, *New Scientist*, 1681, 9 September 1989.

Du Prel, J. B., G. Hommel, B. Röhrig, and M. Blettner (2009), Confidence interval or *P*-value?: Part 4 of a series on evaluation of scientific publications, *Dtsch Arztebl Int*, *106*, 335–339, doi:10.3238/arztebl.2009.0335.

Erinmez, I. A., J. G. Kappenman, and W. A. Radasky (2002), Management of the geomagnetically induced current risks on the national grid company's electric power transmission system, *J. Atmos. Sol. Terr. Phys.*, *64*, 743–756.

Gaunt, C. T., and G. Coetzee (2007), Transformer failures in regions incorrectly considered to have low GIC-risk, *IEEE PowerTech, Lausanne*, 807–812, doi:10.1109/PCT.2007.4538419.

Gopalswamy, N. (2009), Coronal mass ejections and Space Weather, in *Climate and Weather of the Sun-Earth System (CAWSES)*, edited by T. Tsuda et al., pp. 77–120, TERRAPUB, Tokyo, Japan.

Hapgood, M., and D. J. Knipp (2016), Data citation and availability: Striking a balance between the ideal and the practical, *Space Weather*, *14*, 919–920, doi:10.1002/2016SW001553.

Howard, T. (2011), *Coronal Mass Ejections: An Introduction*, Springer-Verlag, New York.

Ingham, M. (1993), Analysis of variations in cathodic protection potential and corrosion risk on the natural gas pipeline at Dannevirke, Report prepared for Natural Gas Corporation, January 1993.

Koen, J., and T. Gaunt (2003), Geomagnetically induced current in the Southern African electricity transmission network, Power Tech Conference Proceedings, 2003 IEEE Bologna, doi:10.1109/PTC.2003.1304165.

Liu, C. M., L. G. Liu, and R. Pirjola (2009), Geomagnetically induced currents in the high-voltage power grid in China, *IEEE Trans. Power Delivery*, *24*, 4.

Liu, L.-G., C.-M. Liu, B. Zhang, Z.-Z. Wang, X.-N. Xiao, and L.-Z. Han (2008), Strong magnetic storm's influence on China's Guangdong power grid, *Chin. J. Geophys.*, *51*(4), 694–699.

Lotz, S. I., M. Heyns, and P. J. Cilliers (2016), Regression-based forecast model of induced geo-electric field, *Space Weather*, *14*, 180–191, doi:10.1002/2016SW001518.

Mäkinen, T. (1993), Geomagnetically induced currents in the Finnish power transmission system, *Finn. Meteorol. Inst. Geophys. Publ.*, *32*.

Martin, B. R. (2012), *Statistics for Physical Sciences*, Academic Press, Oxford, U. K., doi:10.1016/B978-0-12-387760-4.00010-X.

Marshall, R. A., M. Dalzell, C. L. Waters, P. Goldthorpe, and E. A. Smith (2012), Geomagnetically induced currents in the New Zealand power network, *Space Weather*, *10*, S08003, doi:10.1029/2012SW000806.

Pirjola, R. (2008), Study of effects of changes of earthing resistances on geomagnetically induced currents in an electric power transmission system, *Radio Sci.*, *43*, RS1004, doi:10.1029/2007RS003704.

Rajgor, G. (2013), HVDC breakthrough heralds a new era for renewables, *Renew. Energy Focus*, *14*(2), 16–18, doi:10.1016/S1755-0084(13)70026-7.

Rodger, C. J., K. Cresswell-Moorcock, and M. A. Clilverd (2016), Nature's grand experiment: Linkage between magnetospheric convection and the radiation belts, *J. Geophys. Res. Space Physics*, *121*, 171–189, doi:10.1002/2015JA021537.

Rodgers, J. L., and W. A. Nicewander (1988), Thirteen ways to look at the correlation coefficient, *Am. Stat.*, *42*(1), 59–66.

Söderberg, L., and B. Abrahamsson (2001), SwePol link sets new environmental standard for HVDC transmission, *ABB Rev.*, *4*, 62–70.

Thomson, A. W. P., A. J. McKay, E. Clarke, and S. J. Reay (2005), Surface electric fields and geomagnetically induced currents in the Scottish power grid during the 30 October 2003 geomagnetic storm, *Space Weather*, *3*, S11002, doi:10.1029/2005SW000156.

Thomson, A. W. P., E. B. Dawson, and S. J. Reay (2011), Quantifying extreme behavior in geomagnetic activity, *Space Weather*, *9*, S10001, doi:10.1029/2011SW000696.

Transpower (2010), Transpower NZ LTD, asset management plan, April. [Available at https://www.transpower.co.nz/sites/default/files/publications/resources/asset-management-plan-apr-2010.pdf.]

Transpower (2013), HVDC fleet strategy, TP.FS 46.01, 1, October. [Available at https://www.transpower.co.nz/sites/default/files/uncontrolled_docs/Fleet%20Strategy%20-%20HVDC.pdf.]

Trichtchenko, L., and D. H. Boteler (2006), Response of power systems to the temporal characteristics of geomagnetic storms, Canadian Conference on Electrical and Computer Engineering, Inst. of Electr. and Electron. Eng., Ottawa, doi:10.1109/CCECE.2006.277733.

Trivedi, N. B., et al. (2007), Geomagnetically induced currents in an electric power transmission system at low latitudes in Brazil: A case study, *Space Weather*, *5*, S04004, doi:10.1029/2006SW000282.

Viljanen, A., and R. Pirjola (1994), Geomagnetically induced currents in the Finnish high-voltage power system, *Surv. Geophys.*, *15*, 383–408, doi:10.1007/BF00665999.

Viljanen, A., H. Nevanlinna, K. Pajunpää, and A. Pulkkinen (2001), Time derivative of the horizontal geomagnetic field as an activity indicator, *Ann. Geophys.*, *19*, 1107–1118.

Viljanen, A., A. Pulkkinen, R. Pirjola, K. Pajunpää, P. Posio, and A. Koistinen (2006), Recordings of geomagnetically induced currents and a nowcasting service of the Finnish natural gas pipeline system, *Space Weather*, *4*, S10004, doi:10.1029/2006SW000234.

Viljanen, A. (1998), Relation of geomagnetically induced currents and local geomagnetic variations, *IEEE Trans. Power Delivery*, *13*, 1285–1290.

Watari, S., et al. (2009a), Measurements of geomagnetically induced current in a power grid in Hokkaido, Japan, *Space Weather*, *7*, S03002, doi:10.1029/2008SW000417.

Watari, S., et al. (2009b), Correction to "measurements of geomagnetically induced current in a power grid in Hokkaido, Japan", *Space Weather*, *7*, S05099, doi:10.1029/2009SW000484.